

# Evolution of Wurtzite Structured GaAs Shells Around InAs Nanowire Cores

M. Paladugu · J. Zou · Y. N. Guo ·  
X. Zhang · H. J. Joyce · Q. Gao ·  
H. H. Tan · C. Jagadish · Y. Kim

Received: 20 January 2009 / Accepted: 22 April 2009 / Published online: 6 May 2009  
© to the authors 2009

**Abstract** GaAs was radially deposited on InAs nanowires by metal–organic chemical vapor deposition and resultant nanowire heterostructures were characterized by detailed electron microscopy investigations. The GaAs shells have been grown in wurtzite structure, epitaxially on the wurtzite structured InAs nanowire cores. The fundamental reason of structural evolution in terms of material nucleation and interfacial structure is given.

**Keywords** Nanowire heterostructures · GaAs/InAs · Crystal structure

## Introduction

Semiconductor nanowires and their associated heterostructures are ideal candidates to achieve one-dimensional quantum confinement in materials, and thereby they are ideal candidates to explore the physical properties of

materials in one-dimension [1, 2]. Promising physical properties and wide variety of applications were demonstrated using these semiconductor nanostructures [1, 2]. Many nanowire based devices have been demonstrated, including nanowire diodes [3], photodiodes [4], single-electron transistors [5], and field-effect transistors [6, 7]. Various mechanisms have been used to synthesize these semiconductor nanowires, such as vapor–liquid–solid (VLS), vapor–solid, oxide-assisted and solution–liquid–solid [8]. Nanowires growth via the VLS mechanism [9] offers the opportunity to produce axial [10, 11], radial [12, 13], and branched [14] nanowire heterostructures with control over the nanowire size, shape, and location [15]. As a consequence, VLS mechanism has been the most widely used mechanism for nanowires growth. Radial nanowire heterostructures which consist of core, shell, and multi-shell morphologies, offer the flexibility to tailor the band-gap structure of radial nanowire heterostructures [16]. Such flexibility can be used to tune the desired electrical and optical properties.

Many semiconductors of III–V and II–VI compounds can adopt the polytypism of zinc-blende/wurtzite crystal structures based on their growth conditions and difference in the internal energies of two crystal structures for a specific material [17, 18]. These crystal structures differ by the stacking sequence of their dense atomic planes. Zinc-blende structure has ...ABCABC... stacking sequence along  $\langle 111 \rangle$  directions, whereas wurtzite structure has ...ABABAB... stacking sequence along  $\langle 0001 \rangle$  directions. This polytypism gives rise to different band structures depending upon its crystal structure, which, in turn, allows the realization of polytype superlattice structures [19, 20]. Polytypism is often observed when these semiconductors grown in the form of nanowires, especially using Au nanoparticle catalysts. For example, InAs nanowires grown

M. Paladugu · J. Zou · Y. N. Guo · X. Zhang  
School of Engineering, The University of Queensland, Brisbane,  
QLD 4072, Australia

J. Zou (✉)  
Centre for Microscopy and Microanalysis, The University of  
Queensland, Brisbane, QLD 4072, Australia  
e-mail: j.zou@uq.edu.au

H. J. Joyce · Q. Gao · H. H. Tan · C. Jagadish  
Department of Electronic Materials Engineering, Research  
School of Physics and Engineering, The Australian National  
University, Canberra, ACT 0200, Australia

Y. Kim  
Department of Physics, Dong-A University, Hadan-2-dong,  
Saha-gu, Busan 604-714, Korea

via metal–organic chemical vapor deposition (MOCVD) method generally show wurtzite structure, whereas, GaAs nanowires retain its bulk zinc-blende crystal structure [11, 14]. GaAs is a wide bandgap semiconductor material, and InAs has a narrow bandgap. Since the nanowires can act as ideal one-dimensional materials, novel physical properties can be achieved when InAs nanowires sheathed with GaAs. The resultant GaAs/InAs core/shell nanowire structures can give interesting optical and electronic properties of interest to device applications. Since both the semiconductor materials show different crystal structures when they grow axially, it will be scientifically important and technologically necessary to explore how they behave when they grow laterally.

In this study, we grow InAs/GaAs core–shell structures using MOCVD method. They are characterized by detailed transmission electron microscopy (TEM), in terms of their compositional and structural characteristics.

## Experimental

InAs/GaAs core/shell nanowire heterostructures were grown in a horizontal flow MOCVD reactor at 100 mbar with a growth temperature of 450 °C. Firstly, InAs nanowires were grown for 30 min on a GaAs (1̄1̄1) substrate using Au catalysts with a nominal size of ~30 nm by flowing trimethylindium (TMI) and AsH<sub>3</sub>. GaAs is then deposited on these nanowires for 30 min by switching off the TMI flow and switching on the trimethylgallium (TMG) flow. Flow rates of TMI, TMG, and AsH<sub>3</sub> are  $1.2 \times 10^{-5}$ ,  $1.2 \times 10^{-5}$ , and  $5.4 \times 10^{-4}$  mol/min, respectively. The fabricated nanowire heterostructures were characterized by scanning electron microscopy (SEM, JEOL 890) and TEM [Tecnai F20]. TEM specimens were prepared by ultrasonication of the nanowires in ethanol for 10 min followed by dispersal onto holey carbon films.

## Results and Discussion

Figure 1 shows a typical SEM image of GaAs/InAs nanowire heterostructures, in which almost all nanowires grew perpendicular to the substrate surface, i.e., along the [1̄1̄] direction. The nanowires are tapered, suggesting that lateral growth has taken place, particularly in the bottom region [21]. The inset of Fig. 1 is a TEM image of the top portion of a typical GaAs/InAs nanowire and shows the detailed morphology of the GaAs/InAs nanowire with a Au catalyst at the tip. Since GaAs was deposited for 30 min, it is anticipated that GaAs lateral growth has taken place around the InAs nanowires. To understand the lateral growth behavior of GaAs around InAs nanowires, TEM

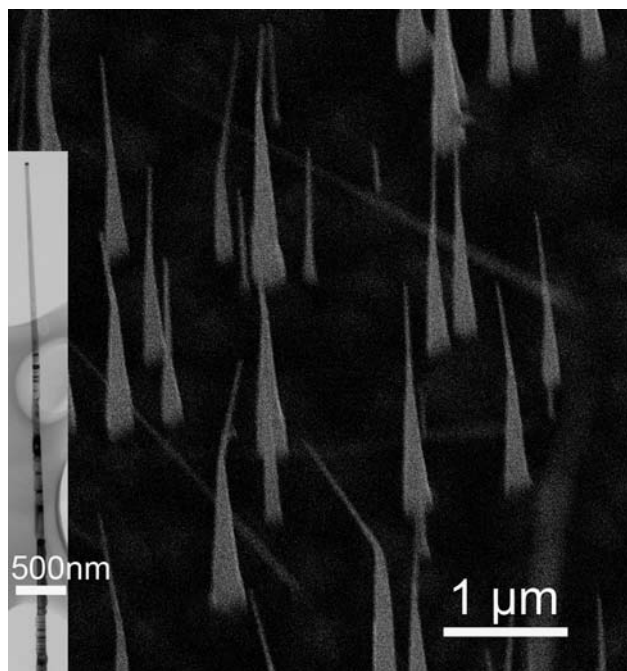
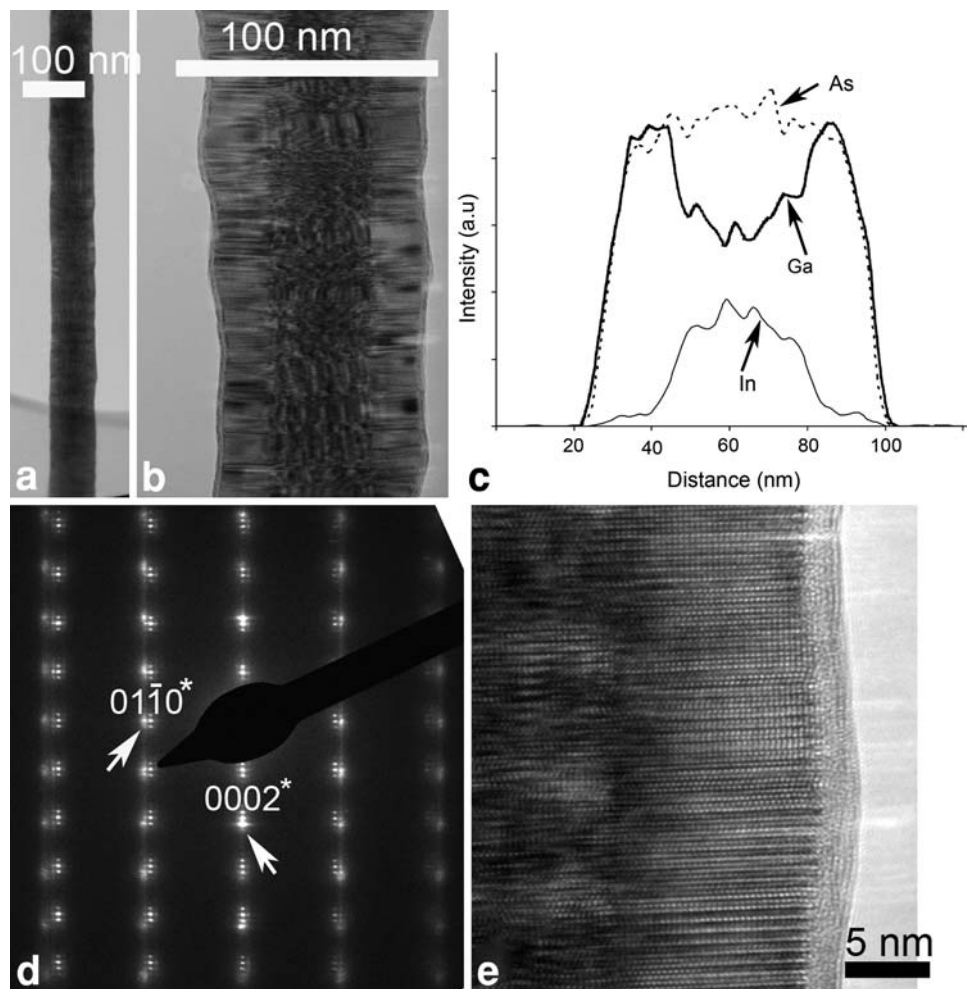


**Fig. 1** SEM image of GaAs/InAs nanowire heterostructures, where the substrate normal is tilted 10° away from the incident electron beam direction. Inset shows a TEM image of the top portion of a typical GaAs/InAs nanowire

investigations were conducted. Figure 2a shows a TEM image of GaAs/InAs radial nanowire heterostructure with a high-magnification image in Fig. 2b. The Moiré fringes in the middle region and stain contrast in the outer region suggest the core/shell structure. To determine the chemical compositional characteristics, energy dispersive spectroscopy (EDS) analysis was performed. Figure 2c shows the qualitative analysis of EDS line scan across the nanowire, clearly showing the InAs/GaAs core/shell nanowire heterostructure. This EDS analysis shows more quantity of Ga than In in the core region. We anticipate that such difference in the quantity is due to higher volume of GaAs shell than the InAs core. In order to determine the structural characteristics of these nanowire heterostructures, electron diffraction is performed. Figure 2d shows a selective area electron diffraction pattern taken from one of these nanowires. Two sets of wurtzite diffraction patterns (along [2̄110] zone axis) with their diffraction spots accompanied by additional double diffraction spots can be seen. This result suggests that both the GaAs and InAs have the wurtzite structure. The lattice mismatch between two sets of diffraction spots can be measured to be  $\sim 6.5 \pm 0.5\%$  in both the axial and lateral directions, suggesting that the misfit strain between the two materials is almost relaxed in both axial and lateral directions and there is no lattice distortion. To further determine the structural characteristics at atomic level, high-resolution TEM (HRTEM) was

**Fig. 2** **a** Low magnification TEM images of a GaAs/InAs nanowire heterostructure. **b** A high-magnification TEM image of the GaAs/InAs nanowire, and its corresponding EDS line-scan spectrum across the nanowire is shown in **(c)**. **d** An electron diffraction pattern taken on the GaAs/InAs core/shell structure. **e** High resolution TEM image showing GaAs/InAs interface region



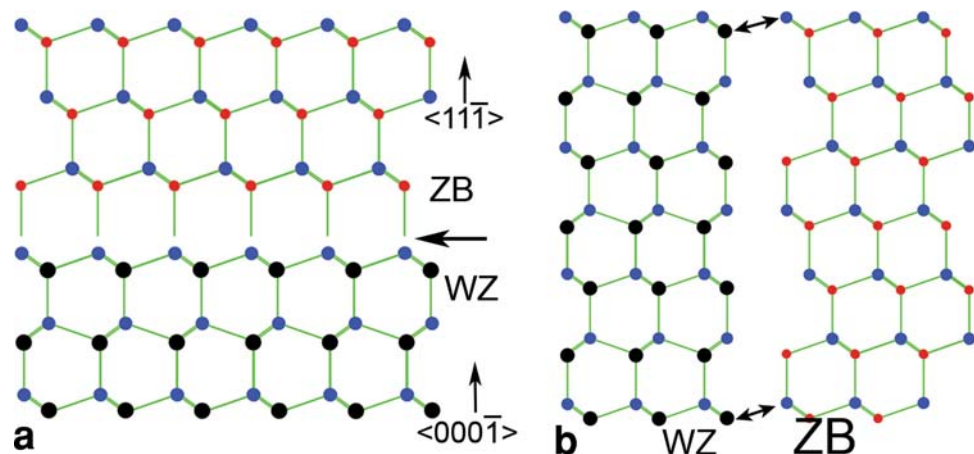
conducted. Figure 2e shows a high-resolution image of the InAs–GaAs core–shell structure. InAs core region can be identified by the presence of the strain contrast, and both the InAs core and the GaAs shell have the wurtzite structure.

As mentioned earlier, InAs nanowires grown along  $\langle 111 \rangle_B$  directions using MOCVD adopt the wurtzite structure. However, when GaAs nanowires grow axially they preserve its bulk crystal structure, the zinc-blende structure. In fact, when InAs and GaAs were grown alternately along the  $\langle 111 \rangle$  directions to form axial nanowire heterostructures, they were observed to have alternating between wurtzite and zinc-blende crystal structures, respectively [11]. However, the results shown in this study and references [12, 13] show that when InAs is sheathed around GaAs nanowires, the sheathed InAs adopt the zinc-blende structure; while when GaAs is sheathed over the InAs nanowires, the sheathed GaAs adopt the wurtzite structure. In order to understand this structural difference between the axial and radial heterostructures, we verify the lattice registry between zinc-blende and wurtzite crystal structures by placing both the structures axially and

laterally. Figure 3a shows  $\langle 1\bar{1}0 \rangle$  projected zinc-blende structure of GaAs placed above the  $\langle \bar{2}110 \rangle$  projected wurtzite structure of InAs. Figure 3b shows both the atomic structures when placed laterally to each other. As can be seen from Fig. 3a, when these structures are placed one another along the  $\langle 111 \rangle$  direction, they can have a lattice registry between them. In fact, both wurtzite and zinc-blende structures are stack of  $\{111\}$  or  $\{0001\}$  planes with a difference in the stacking sequence. Since the atomic arrangements in both  $\{111\}$  and  $\{0001\}$  planes are identical, they can coexist when the nanowires grow in  $\langle 111 \rangle$  or  $\{0001\}$  directions with a lattice registry between the two structures. Such a possibility is believed to be the reason for the coexistence of both wurtzite and zinc-blende structures even in two-dimensions when they grow in  $\langle 111 \rangle$  direction [22].

In the case of lateral direction (Fig. 3b) on the other hand, both crystal structures cannot have a lattice registry except for each sixth layer, as shown by the arrows. In fact, lack of this lattice registry would cause high energy heterointerfaces, and it is observed that such energetic conditions would transform the wurtzite

**Fig. 3** **a** A schematic diagram showing  $\langle\bar{1}\bar{1}0\rangle$  projected zinc-blende structure placed above the  $\langle2\bar{1}10\rangle$  projected wurtzite structure, and **b** shows both the structures but placed in the lateral direction



structure into zinc-blende structure when the wurtzite nanowires are sheathed with two-dimensional zinc-blende layers [23]. Similarly, in our current study, the normally zinc-blende GaAs structure transforms into a wurtzite structure when brought into contact with the InAs NW side walls, by nucleating epitaxially on the nanowire sidewalls.

## Conclusions

We have grown InAs/GaAs core/shell structures using MOCVD method, and the transmission electron microscopy investigations show that both the core and shell contain wurtzite structure. In contrast, when InAs/GaAs heterostructures grow in  $\langle111\rangle$  or  $\langle0001\rangle$  axial directions, both the materials can have different crystal structures. This structural difference between both the axial and lateral direction is explained in terms of crystallography and interfacial structure.

**Acknowledgments** The Australian Research Council is acknowledged for the financial support of this project. M. Paladugu acknowledges the support of an International Postgraduate Research Scholarship. The Australian National Fabrication Facility established under the Australian Government's National Collaborative Research Infrastructure Strategy is gratefully acknowledged for access to the facilities used in this study.

## References

1. H.J. Fan, P. Werner, M. Zacharias, *Small* **2**, 700 (2006). doi: [10.1002/smll.200500495](https://doi.org/10.1002/smll.200500495)
2. A.J. Mieszawska, R. Jalilian, G.U. Sumanasekera, F.P. Zamborini, *Small* **3**, 722 (2007). doi: [10.1002/smll.200600727](https://doi.org/10.1002/smll.200600727)
3. O. Hayden, G.F. Zheng, P. Agarwal, C.M. Lieber, *Small* **3**, 2048 (2007). doi: [10.1002/smll.200700600](https://doi.org/10.1002/smll.200700600)
4. C.J. Novotny, E.T. Yu, P.K.L. Yu, *Nano Lett.* **8**, 775 (2008). doi: [10.1021/nl072372c](https://doi.org/10.1021/nl072372c)
5. H.A. Nilsson, T. Duty, S. Abay, C. Wilson, J.B. Wagner, C. Thelander, P. Delsing, L. Samuelson, *Nano Lett.* **8**, 872 (2008). doi: [10.1021/nl0731062](https://doi.org/10.1021/nl0731062)
6. O. Hayden, M.T. Bjork, H. Schmid, H. Riel, U. Drechsler, S.F. Karg, E. Lortscher, W. Riess, *Small* **3**, 230 (2007). doi: [10.1002/smll.200600325](https://doi.org/10.1002/smll.200600325)
7. S.A. Dayeh, D.P.R. Aplin, X.T. Zhou, P.K.L. Yu, E.T. Yu, D.L. Wang, *Small* **3**, 326 (2007). doi: [10.1002/smll.200600379](https://doi.org/10.1002/smll.200600379)
8. N. Wang, Y. Cai, R.Q. Zhang, *Mater. Sci. Eng. R Rep.* **60**, 1 (2008)
9. R.S. Wagner, W.C. Ellis, *Appl. Phys. Lett.* **4**, 89 (1964). doi: [10.1063/1.1753975](https://doi.org/10.1063/1.1753975)
10. M. Paladugu, J. Zou, Y.N. Guo, G.J. Auchterlonie, Y. Kim, H.J. Joyce, Q. Gao, H.H. Tan, C. Jagadish, *Small* **3**, 1873 (2007). doi: [10.1002/smll.200700222](https://doi.org/10.1002/smll.200700222)
11. M. Paladugu, J. Zou, Y.N. Guo, X. Zhang, Y. Kim, H.J. Joyce, Q. Gao, H.H. Tan, C. Jagadish, *Appl. Phys. Lett.* **93**, 101911 (2008). doi: [10.1063/1.2978959](https://doi.org/10.1063/1.2978959)
12. M. Paladugu, J. Zou, Y.N. Guo, X. Zhang, H.J. Joyce, Q. Gao, H.H. Tan, C. Jagadish, Y. Kim, *Appl. Phys. Lett.* **93**, 201908 (2008). doi: [10.1063/1.3033551](https://doi.org/10.1063/1.3033551)
13. M. Paladugu, J. Zou, Y.N. Guo, X. Zhang, H.J. Joyce, Q. Gao, H.H. Tan, C. Jagadish, Y. Kim, *Angew. Chem. Int. Ed. Engl.* **48**, 780 (2009). doi: [10.1002/anie.200804630](https://doi.org/10.1002/anie.200804630)
14. M. Paladugu, J. Zou, G.J. Auchterlonie, Y.N. Guo, Y. Kim, H.J. Joyce, Q. Gao, H.H. Tan, C. Jagadish, *Appl. Phys. Lett.* **91**, 133115 (2007). doi: [10.1063/1.2790486](https://doi.org/10.1063/1.2790486)
15. M.T. Borgstrom, G. Immink, B. Ketelaars, R. Algra, E. Bakkers, *Nat. Nanotechnol.* **2**, 541 (2007). doi: [10.1038/nnano.2007.263](https://doi.org/10.1038/nnano.2007.263)
16. F. Qian, Y. Li, S. Gradecak, D.L. Wang, C.J. Barrelet, C.M. Lieber, *Nano Lett.* **4**, 1975 (2004). doi: [10.1021/nl0487774](https://doi.org/10.1021/nl0487774)
17. T. Ito, *Jpn. J. Appl. Phys. Part 2 – Lett.* **37**, L1217 (1998)
18. M.I. McMahon, R.J. Nelmes, *Phys. Rev. Lett.* **95**, 215505 (2005). doi: [10.1103/PhysRevLett.95.215505](https://doi.org/10.1103/PhysRevLett.95.215505)
19. M. Murayama, T. Nakayama, *Phys. Rev. B* **49**, 4710 (1994). doi: [10.1103/PhysRevB.49.4710](https://doi.org/10.1103/PhysRevB.49.4710)
20. Z.G. Chen, J. Zou, G. Liu, X.D. Yao, F. Li, X.L. Yuan, T. Sekiguchi, G.Q. Lu, H.M. Cheng, *Adv. Funct. Mater.* **18**, 3063 (2008). doi: [10.1002/adfm.200800447](https://doi.org/10.1002/adfm.200800447)
21. J. Zou, M. Paladugu, H. Wang, G.J. Auchterlonie, Y.N. Guo, Y. Kim, Q. Gao, H.J. Joyce, H.H. Tan, C. Jagadish, *Small* **3**, 389 (2007). doi: [10.1002/smll.200600503](https://doi.org/10.1002/smll.200600503)
22. V.V. Chaldyshev, B. Nielsen, E.E. Mendez, Y.G. Musikhin, N.A. Bert, Z. Ma, T. Holden, *Appl. Phys. Lett.* **86**, 131916 (2005). doi: [10.1063/1.1875759](https://doi.org/10.1063/1.1875759)
23. G. Patriarche, F. Glas, M. Tchernycheva, C. Sartel, L. Largeau, J.C. Harmand, *Nano Lett.* **8**, 1638 (2008). doi: [10.1021/nl080319y](https://doi.org/10.1021/nl080319y)